



A versatile AIE fluorogen with selective reactivity to primary amines for monitoring amination, protein labeling, and mitochondrial staining

Xinyuan He, Huilin Xie, Lianrui Hu, Pengchao Liu, Changhuo Xu, Wei He, Wutong Du, Siwei Zhang, Hao Xing, Xinyue Liu, et al.

► To cite this version:

Xinyuan He, Huilin Xie, Lianrui Hu, Pengchao Liu, Changhuo Xu, et al.. A versatile AIE fluorogen with selective reactivity to primary amines for monitoring amination, protein labeling, and mitochondrial staining. Aggregate, 2022, 10.1002/agt2.239 . hal-03807047

HAL Id: hal-03807047

<https://hal.science/hal-03807047>

Submitted on 8 Oct 2022

HAL is a multi-disciplinary open access archive for the deposit and dissemination of scientific research documents, whether they are published or not. The documents may come from teaching and research institutions in France or abroad, or from public or private research centers.

L'archive ouverte pluridisciplinaire **HAL**, est destinée au dépôt et à la diffusion de documents scientifiques de niveau recherche, publiés ou non, émanant des établissements d'enseignement et de recherche français ou étrangers, des laboratoires publics ou privés.

A versatile AIE fluorogen with selective reactivity to primary amines for monitoring amination, protein labeling, and mitochondrial staining

Xinyuan He¹  | Huilin Xie¹ | Lianrui Hu¹ | Pengchao Liu² | Changhuo Xu¹ | Wei He¹ | Wutong Du¹ | Siwei Zhang¹ | Hao Xing¹ | Xinyue Liu¹ | Hojeong Park¹ | Tsz Shing Cheung¹ | Min-Hui Li³ | Ryan T. K. Kwok^{1,4} | Jacky W. Y. Lam^{1,4} | Jian Lu² | Ben Zhong Tang^{1,4,5,6} 

¹Department of Chemistry, Hong Kong Branch of Chinese National Engineering Research Center for Tissue Restoration and Reconstruction, State Key Laboratory of Molecular Neuroscience, Division of Life Science and Department of Chemical and Biological Engineering, The Hong Kong University of Science and Technology, Kowloon, Hong Kong, China

²Department of Mechanical Engineering, City University of Hong Kong, Greater Bay Joint Division, Shenyang National Laboratory for Materials Science, Kowloon, Hong Kong, China

³Chimie ParisTech PSL University Paris, CNRS, Institut de Recherche de Chimie Paris, Paris, France

⁴Department of Chemistry, Guangdong-Hongkong-Macau Joint Laboratory of Optoelectronic and Magnetic Functional Materials, The Hong Kong University of Science and Technology, Kowloon, Hong Kong, China

⁵Center for Aggregation-Induced Emission, SCUT-HKUST Joint Research Institute, State Key Laboratory of Luminescent Materials and Devices, South China University of Technology, Guangzhou, China

⁶School of Science and Engineering, Shenzhen Key Laboratory of Functional Aggregate Materials, The Chinese University of Hong Kong, Shenzhen City, Guangdong, China

Correspondence

Jian Lu, Department of Mechanical Engineering, City University of Hong Kong, Greater Bay Joint Division, Shenyang National Laboratory for Materials Science, Tat Chee Avenue, Kowloon, Hong Kong, China.
Email: jianlu@cityu.edu.hk

Ben Zhong Tang, Department of Chemistry, Hong Kong Branch of Chinese National Engineering Research Center for Tissue Restoration and Reconstruction, State Key Laboratory of Molecular Neuroscience, Division of Life Science and Department of Chemical and Biological Engineering, The Hong Kong University of Science and Technology, Clear Water Bay, Kowloon, Hong Kong, China.
Email: tangbenz@cuhk.edu.cn

Xinyuan He, Huilin Xie, and Lianrui Hu contributed equally to this work.

Funding information

National Natural Science Foundation of China, Grant/Award Number: 21788102; Research Grants Council of Hong Kong, Grant/Award Numbers: 16307020, 16306620, 16305518, N_HKUST609/19, C6009-17G, C6014-20w; Innovation and Technology Commission, Grant/Award Numbers: ITC-CNERC14SC01, ITCPD/17-9; Natural Science Foundation of Guangdong Province, Grant/Award Number: 201913121205002

Abstract

Specific bioconjugation for native primary amines is highly valuable for both chemistry and biomedical research. Despite all the efforts, scientists lack a proper strategy to achieve high selectivity for primary amines, not to mention the requirement of fast response in real applications. Herein, we report a chromone-based aggregation-induced emission (AIE) fluorogen called CMVMN as a self-reporting bioconjugation reagent for selective primary amine identification, and its applications for monitoring bioprocesses of amination and protein labeling. CMVMN is AIE-active and capable of solid-state sensing. Thus, its electrospun films are manufactured for visualization of amine diffusion and leakage process. CMVMN also shows good biocompatibility and potential mitochondria-staining ability, which provides new insight for organelle-staining probe design. Combined with its facile synthesis and good reversibility, CMVMN would not only show wide potential applications in biology, but also offer new possibilities for molecular engineering.

KEY WORDS

aggregation-induced emission (AIE), bioconjugation, mitochondria-staining, primary amines, protein labeling

This is an open access article under the terms of the [Creative Commons Attribution](#) License, which permits use, distribution and reproduction in any medium, provided the original work is properly cited.

© 2022 The Authors. *Aggregate* published by SCUT, AIEI, and John Wiley & Sons Australia, Ltd.

1 | INTRODUCTION

In situ probe of biomolecules has become a new pursuit for scientists due to its increasing impact on studying cellular processes and therapeutic applications.^[1,2] The assignment of the 2008 Nobel Prize in Chemistry to genetically encoded fluorescent proteins is a good example.^[3] However, cellular systems are full of biological electrophiles and nucleophiles, and no such tools as fluorescent proteins can be used for non-proteinaceous targets.^[4] To deal with this problem, orthogonal bioconjugation was coined in 2013,^[5] which refers to selective chemical reactions in living systems.^[6] It has brought a fabulous success in selective labeling of biomolecules,^[7–9] but the prefunctionalization of nature substrate with one of the specific reaction handles like alkynes, azides, ketones, and tetrazines is complex.^[10] To monitor the time course of the reaction, an additional indicator is further needed.^[11,12] On the other hand, by means of the advancement of synthetic organic chemistry, it is possible and meaningful to utilize native functional groups as “handles” and self-reporters for in situ and selective bioconjugation.

Amines are ubiquitous in living systems,^[13] making them ideal native candidates for bioconjugation. Nonetheless, the worldwide covalent labeling of amines with compounds bearing isothiocyanate,^[14–16] N-hydroxysuccinimidyl ester,^[17–19] or pen-tafluorophenyl^[20–22] is not applicable for selective bioconjugation due to the similar reactivity with primary amines and secondary amines, and even to some extent interference from thiols and other nucleophiles. Previously, primary amines were reported to show special reactivity toward some electrophiles and light-induced oxidative coupling reagent,^[23–26] which made it even more attractive as a native “handle”. Notably, fast and efficient bioconjugation of activated alkynes and native amines without prefunctionalization was reported by our group.^[27] Encouraged by this success, we are eager to create probes with high affinity, reactivity and selectivity toward primary amines.

Chromone is reactive to amines at high concentration or high temperature. Interestingly, its products with primary amines form a special intramolecular hydrogen bond and become stable, inducing a high affinity toward primary amines.^[28,29] The introduction of a methyl group in α position of the carbonyl group can further affect its reaction with amines to result in enhanced selectivity toward primary amines.^[30] Besides, the discovery of epicocconone, which has a similar conjugate structure for primary amine probing, reminds us the importance of rational molecular design.^[31] So even though none of the reported chromone derivatives can realize fast, selective bioconjugation for primary amines at room temperature,^[28–30,32–34] we believe that when a proper electron withdrawing group is introduced to the α position of chromone, the obtained new compound may be activated and show good affinity and selectivity toward primary amines. Or more, with a similar donor–acceptor structure as epicocconone, the fluorescent signal may be seen as well.

Fluorescence sensing is a non-invasive imaging modality with easy operation and high spatial-temporal resolution.^[35] Traditional organic dyes tend to aggregate and triggers the undesirable aggregation caused quenching effect.^[36] Fortunately, the discovery of a phenomenon of aggregation-

induced emission (AIE) has solved the problem.^[37] AIE fluorogens are weakly emissive in molecularly dissolved state, but become highly emissive in aggregate state, making them as ideal candidates for the observation of bioconjugation procedure.^[38–41] Conceivably, if an AIE fluorogen that undergoes specific reaction with primary amines is developed, its applications will no longer be limited to diluted solutions.

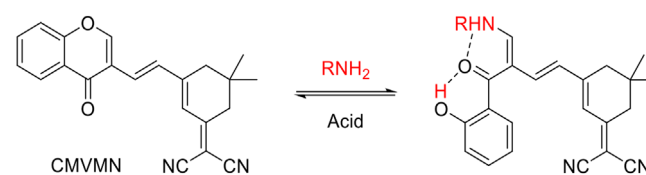
In this work, we introduced a one-step synthesis of (E)-2-{5,5-dimethyl-3-[2-(4-oxo-4H-chromen-3-yl)vinyl]cyclohex-2-en-1-ylidene}malononitrile (abbreviated as CMVMN, Scheme 1) which could undergo selective bioconjugation with primary amines, and showed self-reporting property. The reaction was fast and highly selective. Meanwhile, a distinct color change and fluorescence turn-on signal at 595 nm were both detected, enabling CMVMN to monitor bioprocesses of amination and protein labeling. NMR titration and theoretical calculation were conducted and verified the reaction mechanism. CMVMN was AIE-active and was capable of solid-state sensing. Thus, its electrospun films were fabricated for visualization of amine diffusion and leakage process in a real-time manner. Furthermore, CMVMN showed good biocompatibility and a mitochondria-staining ability.

2 | RESULTS AND DISCUSSION

2.1 | Photophysical properties

CMVMN absorbed at 387 nm (Figure S5) and emitted weakly in THF at 530 nm, with a quantum yield (QY) of 0.3% (Figure 1A). When a poor solvent of deionized water was added, the fluorescence intensity enhanced gradually due to the aggregation of CMVMN molecules. Also, the QY reached 0.7% at water fraction of 95%, verifying its AIE property. However, the fluorescence signal was still very weak, like that of the amorphous powder (QY = 0.5%, Figure 1B and Figure S6A). Curiously, the amorphous powder was cooled down. Distinct orange fluorescence was then observed at 195 K and it became stronger at 77 K (Figure 1B). This indicated the molecule became more emissive once its intramolecular motion was slowed down at low temperature.

The single crystal of CMVMN became highly emissive (Figure 1C and Figure S6B) and its QY (63%) was 126 times higher than that of the amorphous powder. Such a phenomenon was named as “crystallization-induced emission” before.^[42–45] For CMVMN crystals, each molecule formed six hydrogen bonds with surround molecules, which efficiently restricted its intramolecular motion (Figure 1D). The strong intermolecular interactions in the crystal largely



S C H E M E 1 Specific and reversible reaction of CMVMN with primary amines

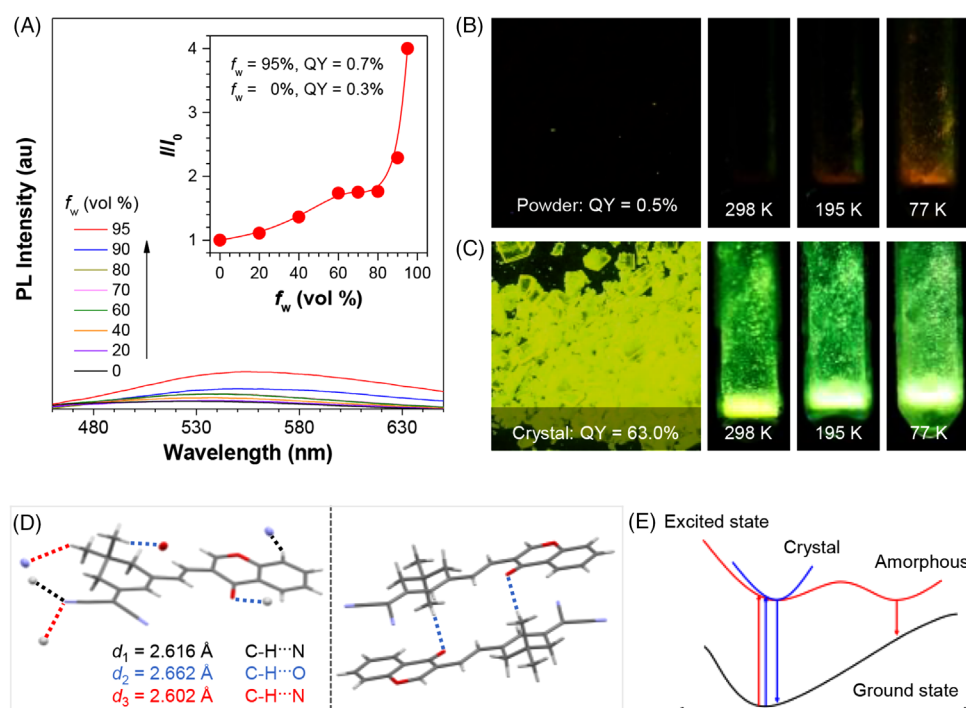


FIGURE 1 (A) Photoluminescence (PL) spectra of CMVMN ($10 \mu\text{M}$) in THF/water mixtures with different water fractions (f_w). Inset: Plot of I/I_0 versus f_w ; I = PL intensity at f_w , I_0 = PL intensity at $f_w = 0\%$. $\lambda_{\text{ex/em}} = 387/550 \text{ nm}$. Fluorescent images of (B) amorphous powder and (C) crystalline solid of CMVMN taken under UV irradiation at 298, 195, and 77 K. (D) Crystal packing of CMVMN molecules. (E) Proposed decay pathways along potential energy surfaces of CMVMN in the crystalline and amorphous states

rigidified the molecular conformation and avoided detrimental π - π interactions, making them show intense crystal-state emission.^[46,47] Meanwhile, the emission maximum in the crystalline state ($\lambda_{\text{em}} = 530 \text{ nm}$, $\tau = 2.12 \text{ ns}$, 77 K) was blue-shifted compared with that of the amorphous state ($\lambda_{\text{em}} = 605 \text{ nm}$, $\tau = 1.06 \text{ ns}$, 77 K) (Figures S7 and S8). Probably, the loose packing in the amorphous state enabled the molecules to undergo some sort of intramolecular motion and hence an excited-state minimum with a small band gap emerged for amorphous sample. Eventually, the red-shifted and weakened emission was observed (see the proposed decay pathways in Figure 1E).^[48] The red-shifted and decreased emission of the crystalline solid in 298 K was also in accordance with this conjecture (Figure 1C and Figure S7A).

2.2 | Reactivity and sensing response

Upon addition of propylamine (PA), the absorption peak at 387 nm decreased, but a new peak emerged at 480 nm (Figure 2A), enabling the direct visualization of the amination process. Meanwhile, a significant fluorescence turn-on signal was detected at 595 nm and the intensity increased by 823 folds at a [PA] of 10 mM , which enabled the sensitive detection of PA (Figure 2B). Quantitative monitoring of PA was performed and a good linear curve was obtained at a concentration range of 0 – 2.0 mM (Figure 2C), from which a detection limit of $4.4 \mu\text{M}$ was calculated.^[49] Moreover, the PA detection was realized via a colorimetric method (Figure S9). Hence, CMVMN could be a fluorescent and colorimetric dual-mode probe for primary amines.

The amination initiated rapidly and the fluorescence signal almost reached a plateau within 5 min at a low PA concentration (1.0 mM) (Figure 2D). The saturation time was further reduced to 1 min at a high PA concentration (5.0 mM). Since nucleophilic reactions were better carried out under alkaline conditions,^[50,51] it illustrated the autocatalytic effect of PA at high concentration. The protonation of PA with trifluoroacetic acid (TFA) would inhibit the amination process to result in decreased fluorescence. In this work, although the amination was well finished before the addition of TFA, decreased fluorescence intensity was observed, revealing the good reversibility of amination process (Figure 2E). Even more, the fluorescence turned out to be controllable via cycle addition of PA or TFA (Figure 2E), making CMVMN a promising tool for long-time dynamic tracking.^[52]

Solid-state sensing is much preferred in real applications thanks to its simple sample preparation.^[53,54] The strong emission of AIEgens in solid-state makes them ideal candidates for such purpose.^[55] Curiously, the spin-coating films of CMVMN was fabricated from its dichloromethane solution and then fumed with PA vapors. A remarkable red-shift emission was observed 1 min later (Figure 2F). The emission peak red-shifted by 50 nm after exposure to PA vapors of low concentration (0.05 mM), indicating the high sensitivity. Also, quantitative detection of PA vapors using the spin-coating films were performed (Figure S10). Moreover, CMVMN exhibited good stability and reversibility after repeated exposure to PA and TFA vapors, as evidenced by the similar spectrum to that of the initial sample from the ^1H NMR measurement (Figures S1 and S11).

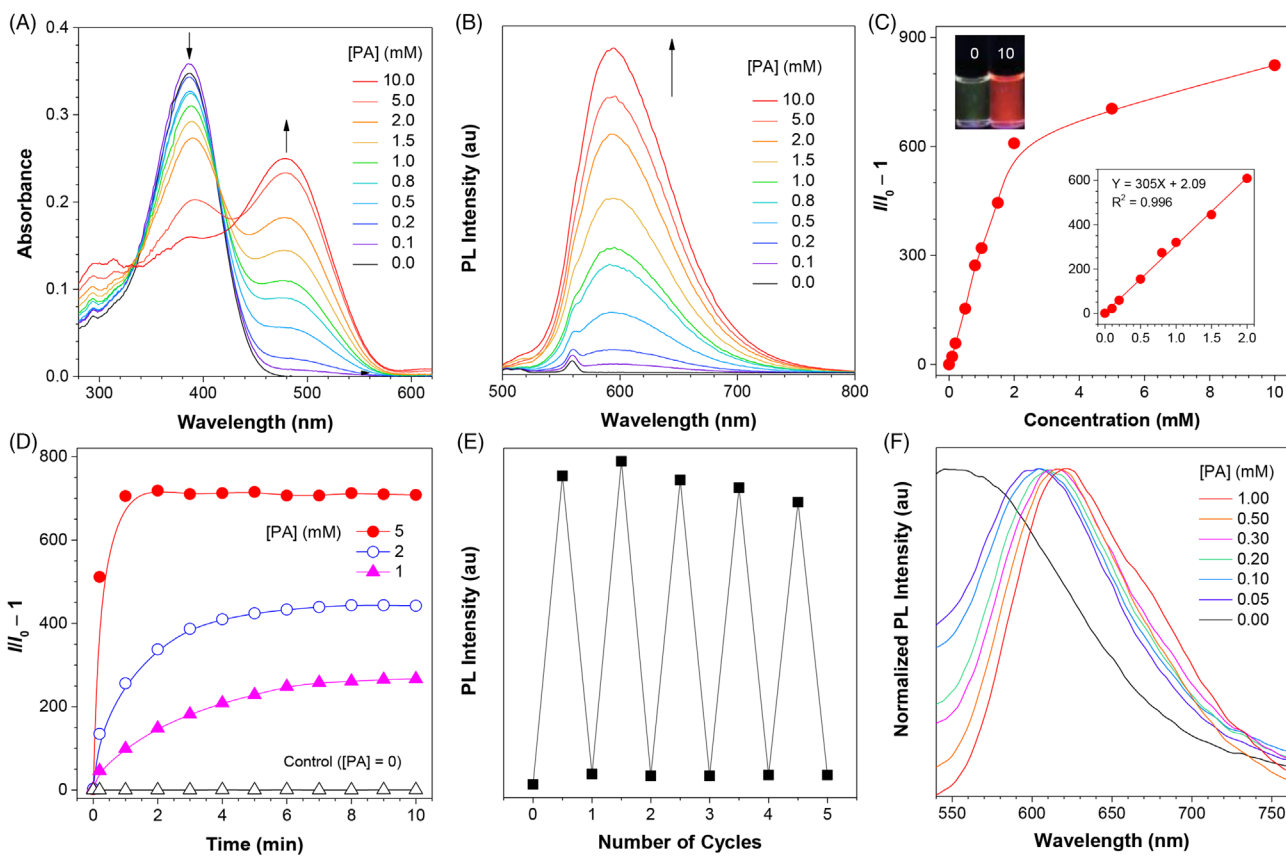


FIGURE 2 Changes in (A) absorption and (B) PL spectra of CMVMN ($10 \mu\text{M}$) with addition of PA in THF solution. (C) Plot of relative fluorescence intensity ($I/I_0 - 1$) versus concentration of PA [PA]. Inset: (upper) Photographs of CMVMN before and after reaction with 10 mM PA taken under UV irradiation; (lower) linear fitting curve of ($I/I_0 - 1$) toward [PA]. (D) Time course of amination reaction of CMVMN by PA. (E) Reversible changes in PL intensity of CMVMN upon repeated exposures to PA and trifluoroacetic acid. (F) Normalized PL spectra of spin-coating films of CMVMN fumed with different amount of PA for 1 min. $\lambda_{\text{ex/em}} = 480/595 \text{ nm}$

2.3 | Selectivity

The fluorescence response of CMVMN to various nucleophiles bearing amido, hydroxyl or sulfhydryl groups was investigated. CMVMN reacted not only with PA, but also other primary amines, as revealed by the emission enhancement (Figure 3). By increasing the steric hindrance (TBA > benzylamine > cyclohexylamine), an obvious decrease in fluorescence was observed, indicating the decisive role of steric effects for amines. If CMVMN was incubated with TBA for a long time, the fluorescence increased gradually but slowly (Figure S12), which further verified the steric effect-caused weak reactivity. Under the same conditions, the fluorescence enhancement effect of primary amines was much bigger than that of other amines such as secondary amines, tertiary amines, heterocyclic amines, aromatic amines and ammonia. Meanwhile, nucleophiles with hydroxyl or sulfhydryl showed no obvious reactivity. These results revealed the high reactivity and selectivity of CMVMN toward primary amines.

2.4 | Reaction mechanism

NMR titration experiments were further conducted. In general, the ^1H NMR spectra of enamines generated from chromones and primary amines showed a characteristic

broad signal at δ 9–12, which attributed to the resonance of an NH group forming a strong intermolecular hydrogen bond.^[28,29] Accordingly, a new broad peak at δ 10.8 emerged in the ^1H NMR spectra of CMVMN after addition of PA and the signal was intensified when more PA was added (Figure S13). Meanwhile, the original conjugated structure of CMVMN was destroyed to result in a decreased deshielding effect on the surrounding hydrogen atoms. Thus, new peaks appeared at lower fields compared with those of CMVMN. Beyond that, a mass peak at mass-to-charge ratio (m/z) of 424.2002 $[\text{M}+\text{Na}]^+$ (Figure S14) related to compound S7 (Scheme 2) was detected. Hereby, CMVMN may follow a reaction path similar to typical chromones.^[28–30]

Later, density functional theory calculation was carried out. The initial nucleophilic attack followed by isomerization formed the intermediate product S3 with a high energy (10.1 kcal/mol, Scheme 2). Followed, the rate-limiting step of bond dissociation taken place accompanied with isomerization to form a metastable intermediate product S5 (3.0 kcal/mol). Since the reaction energy barrier was only 20.7 kcal/mol, the amination of CMVMN with primary amines could happen readily at room temperature. Importantly, the obtained products were stabilized by intramolecular hydrogen bonds and of low energy (−4.8 kcal/mol). However, the story for diethylamine was different (Scheme S2). The reaction energy barrier for

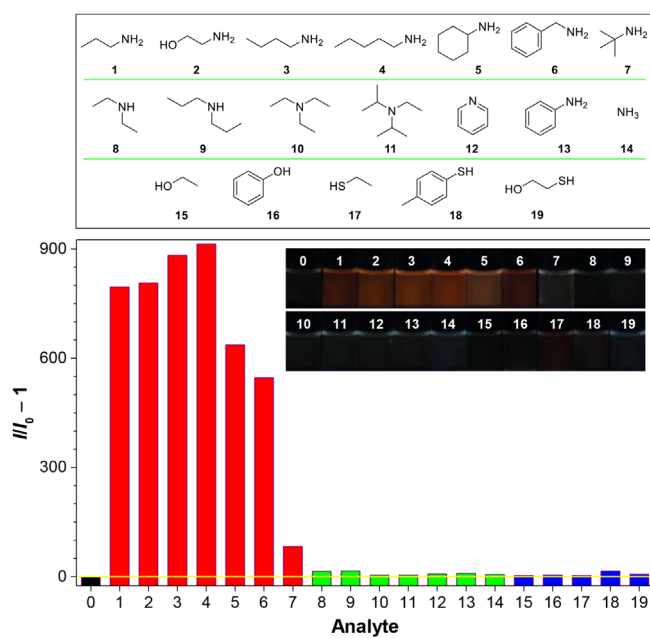


FIGURE 3 (Upper panel) Chemical structures of the analytes investigated in this study. (Lower panel) Relative fluorescence intensity ($\frac{I}{I_0} - 1$) of CMVMN ($10 \mu\text{M}$) after its mixing with different analytes (10 mM) in THF for 10 min. Analytes: [(0) CMVMN (control)], (1) PA, (2) ethanolamine, (3) butylamine, (4) amylamine, (5) cyclohexylamine, (6) benzylamine, (7) TBA, (8) diethylamine, (9) dipropylamine, (10) trimethylamine, (11) *N,N*-diisopropylethylamine, (12) pyridine, (13) aniline, (14) ammonia, (15) ethanol, (16) phenol, (17) ethanethiol, (18) *p*-toluenethiol, and (19) mercaptoethanol. $\lambda_{\text{ex/em}} = 480/595 \text{ nm}$. Inset: fluorescent images of the mixtures of the analytes and CMVMN

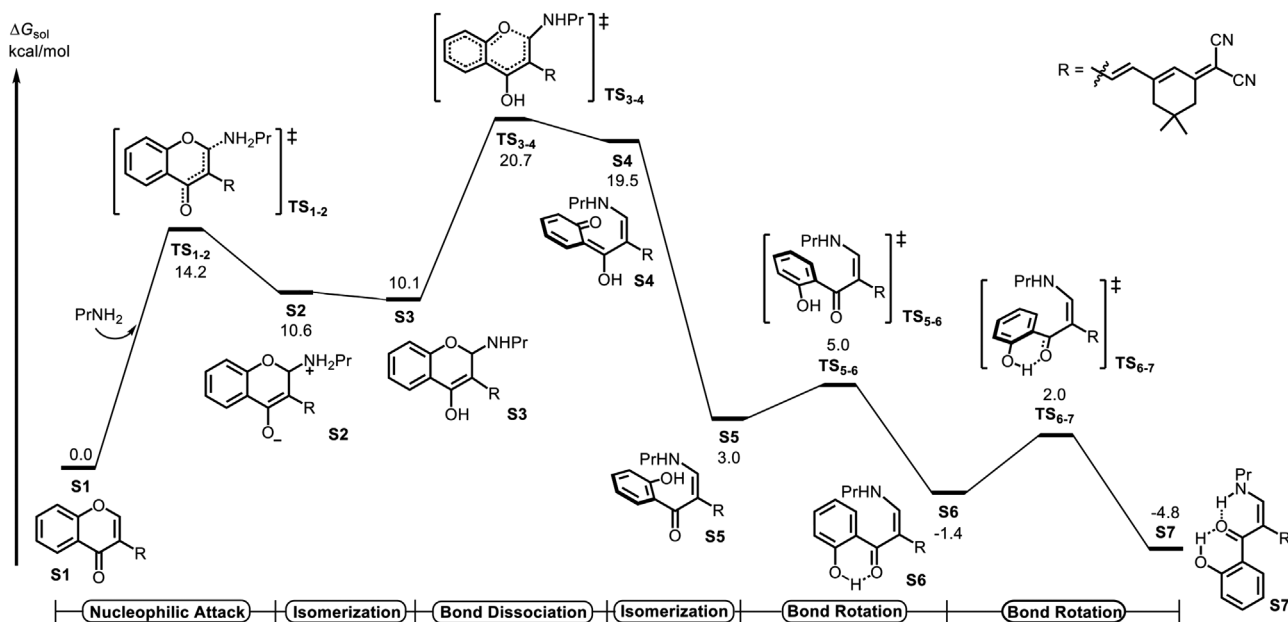
bond dissociation was much higher (29.2 kcal/mol) because of steric effect. Thus, its reaction with CMVMN usually ended after the generation of S9 (12.3 kcal/mol), but even if S12 could be produced, it was unstable and its energy would be relatively higher (5.1 Kcal/mol) than that of S7. Since both S3 and S9 were not stable in view of their high energy, CMVMN is not a good reagent for one-step nucleophilic addition as other reported electrophiles.^[14–22] Overall, the

steric effect impeded the reaction of secondary amines with CMVMN, while the special intramolecular hydrogen bonding in the resulting product contributed to the amination of CMVMN with primary amines, and ultimately achieve the selective bioconjugation of CMVMN with primary amines.

2.5 | Applications in printing

CMVMN was further applied to printing and the “spider-web” sensors were manufactured (Figure S15A). A relatively high thermal decomposition temperature of $T_d = 294^\circ\text{C}$ (Figure S16) was observed via thermo-gravimetric analysis, demonstrating its high thermostability. Besides, the sensor was made up of micro fibers (Figure S15B) and its loose structure was in favor of the fluxion of amine vapors. The initial sensor was pale yellow with yellow-green fluorescence. When fumed with PA, it became orange and emitted a red fluorescence (Figure S17). Obviously, this noticeable change offered a workable method for equipment-free monitoring of primary amines, but such a change was not observed for diethylamine or trimethylamine, indicating the potential of rapid identification of primary amines.

CMVMN also showed a fast and sensitive response to PA vapors (Figure 4A). At the moment PA was added to the container, the color change was detected. Notably, it first took place near the container, and 30 s later, the whole sensor changed (Videos S2 and S3). Clearly, due to the high sensitivity of CMVMN and fast rate of the amination, the diffusion process of PA was successfully visualized and recorded. Further, a PA leakage model was constructed, in which PA was sealed in a culture dish and the sensor was put on top of it, followed by piercing with a needle to make a leaking point. A real-time leaking process was then visualized and the leaking point could be recognized easily (Figure 4B and Videos S4 and S5). However, when the fumed sensor was put in open air, a gradual color fading appeared. It took



SCHM E 2 Energy profile for the reaction pathway of CMVMN with PA

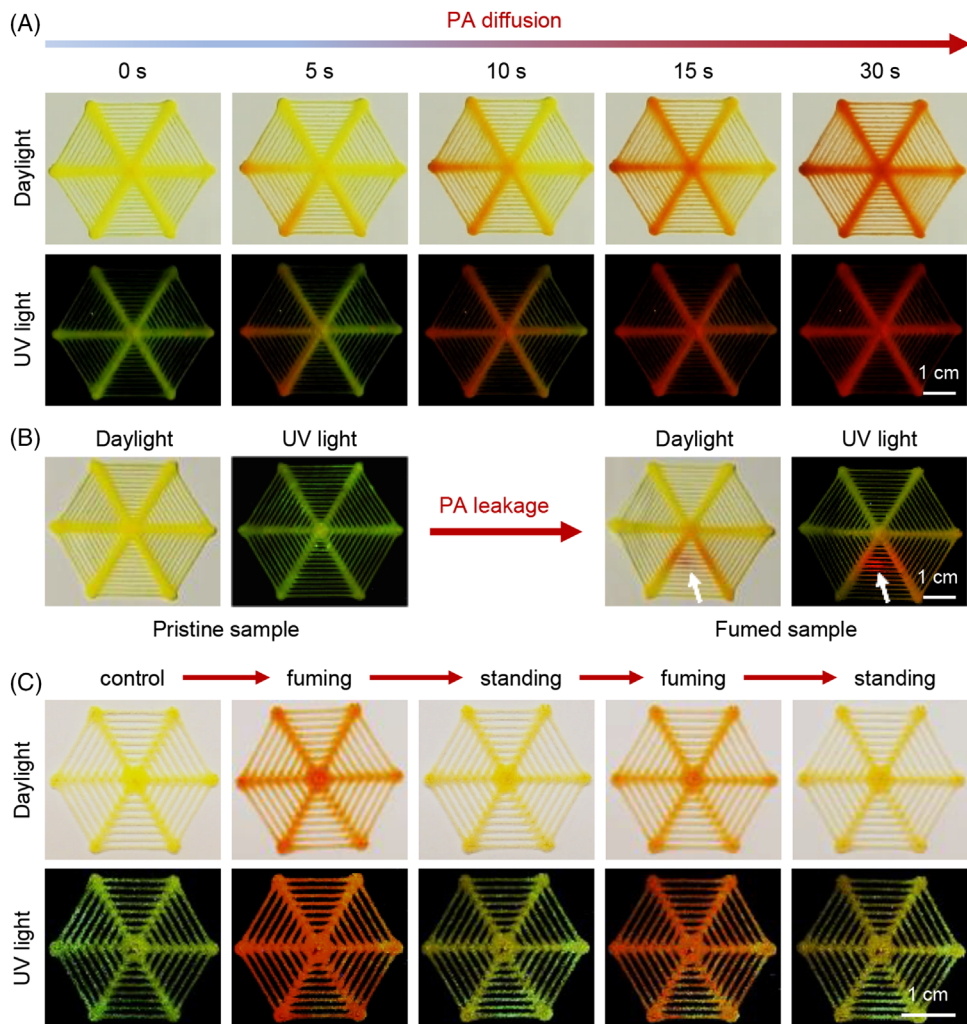


FIGURE 4 Photographs and fluorescence images of (A) the electrospun films of “spider-web” sensors printed from CMVMN microcrystals blended into polycaprolactone matrix upon exposure to PA vapor; (B) demonstration of the CMVMN sensors for the detection of PA leakage (arrow indicating the leaking point). (C) Reversible changes in absorption and emission colors during repeated cycling exposure to PA vapor

about 30 min for the whole fumed sensor to revert to its original state (Figure S18). A similar phenomenon was witnessed for the fumed sensor obtained from the PA leakage model as well (Figure S19). Furthermore, reversible changes in both color and emission were observed for the printing sensor via repeated cycling fuming or standing (Figure 4C), demonstrating the high value of CMVMN for monitoring of leakage.

2.6 | Labeling of biomolecules in aqueous solution

In situ probe of biomolecules was the final and crucial demand for bioconjugations. When numerous small biomolecules were chosen and cultured with CMVMN (Figure 5A), nearly no fluorescence enhancement was detected for CMVMN in the presence of other polar basic (histidine), polar neutral (tryptophan, serine, asparagine, and cysteine), polar acidic (glutamic acid) and nonpolar hydrophobic (alanine) amino acids as well as the important tripeptide glutathione^[56]. In terms of the structural formula, only arginine and lysine possessed reactive residues with the NH₂ group, and the guanidino moiety was called the primary guanidino amine^[57]. Also, the α -amino groups of amino

acids were usually less reactive in nucleophilic bioconjugation due to the interference of the carboxylic acid.^[22,58–60] Thus, the high reactivity of CMVMN with primary amine groups provides a new pathway for specific bioconjugation of lysine and arginine. Additionally, N(α)-Boc-L-arginine was tested and a similar fluorescence response toward CMVMN as arginine was witnessed, proving the importance of the primary guanidino amine for the amination (Figure S20). Moreover, nitrogen bases (thymine, adenine, and cytosine) and monosaccharides (glucose and fructose) were found to be inert to CMVMN. Thus, the selectivity of CMVMN toward specific amino acids (lysine and arginine) could make it a promising candidate for selective labeling of proteins.

Next, the amination process in different pH was investigated. To avoid the deterioration of the activity and structure of biomolecules, mild pH conditions were preferred. CMVMN reacted readily with arginine and lysine under relative alkaline conditions (pH > 7.4), but was greatly inhibited at pH 6.0 (Figure 5B), revealing a tunable amination process. Also, a dramatic change in relative fluorescence intensity was observed from pH 7.0 to 7.8, which suggested that CMVMN might be lighted up in a relative alkaline environment like in the mitochondria of cells. For CMVMN alone, the fluorescence kept almost constant and such a stability was favorable

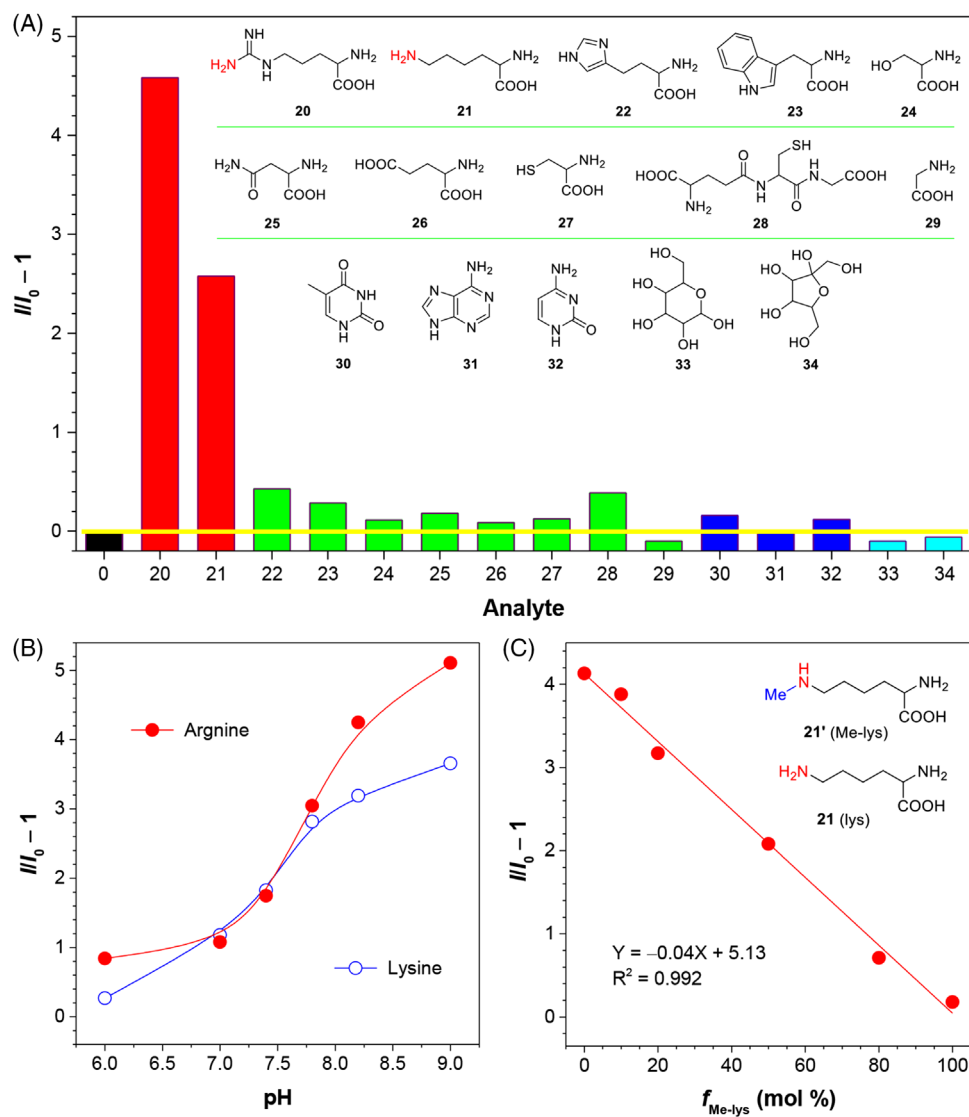


FIGURE 5 (A) Relative fluorescence intensity ($\text{III}_0 - 1$) of CMVMN (10 μM) after mixing with various analytes (10 mM) in PBS for 10 min. Analytes: [(0) CMVMN (control)], (20) arginine, (21) lysine, (22) histidine, (23) tryptophan, (24) serine, (25) asparagine, (26) glutamic acid, (27) cysteine, (28) glutathione, (29) glycine, (30) thymine, (31) adenine, (32) cytosine, (33) glucose, (34) fructose. $\lambda_{\text{ex/em}} = 480/595 \text{ nm}$. (B) Effect of pH on the reaction of CMVMN with arginine (red solid circle) and lysine (blue open circle). (C) Change in fluorescence intensity of CMVMN against the fraction of Me-lys in a mixture of lysine and Me-lys

for sensing and labeling (Figure S21). When N_6 -methyl-L-lysine (Me-lys) was picked up as a model compound to replace some lysine in the same amount, a decreased fluorescence was detected (Figure 5C). A good linearity between the relative fluorescence intensity and $f_{\text{Me-lys}}$ was found as well, which demonstrated the applicability of CMVMN for selective amination of primary amines in aqueous solutions. Meanwhile, it reflected the potential of primary amine selective probes for monitoring methylation, which is an important part of post-translational modifications for proteins.^[61,62]

Interestingly, when HSA was added, the fluorescence spectrum largely intensified and the relative fluorescence intensity was increased by 90 folds (Figure 6A). Such an enhancement effect was noticed to be surprisingly stronger than that of arginine or lysine, especially when the high concentration (10 mM) used for amino acids testing was taken into account. Prior to this, AIEgens were found to be more reactive in cavity due to the restriction of intramolecular motions.^[63] In view of the hydrophobic nature of CMVMN, it may be trapped in the cavity of HSA (Figure S22) to

result in such a significantly enhanced fluorescent signal. At least, the enhanced specificity could make CMVMN more applicable for in situ labeling of biomacromolecules since interference from other small biomolecules became negligible. Identically, because of the difference in the cavity, it was reasonable to see a discrepant selectivity of CMVMN toward other proteins, including BSA, hemoglobin, transferrin, papain, lysozyme, and lipase (Figure 6A).

To get further insight, molecular docking calculations were performed. In the HSA-CMVMN complex, CMVMN was docked in the hydrophobic cleft via the hydrogen bond interaction with ILE-142 (Figure S22). Further, nearest neighbor residues around the ligand were identified and the ARG-117 could be the reaction site in the binding cleft. In the BSA-CMVMN complex, two binding sites were found and both sites exhibited arginine residues around the ligand. However, one of the binding sites was not activated due to the hydrogen bond interactions which locked the aromatic ring and hindered the formation of the transition state (Figure S23). Thus, CMVMN could label BSA, but its reactivity was not

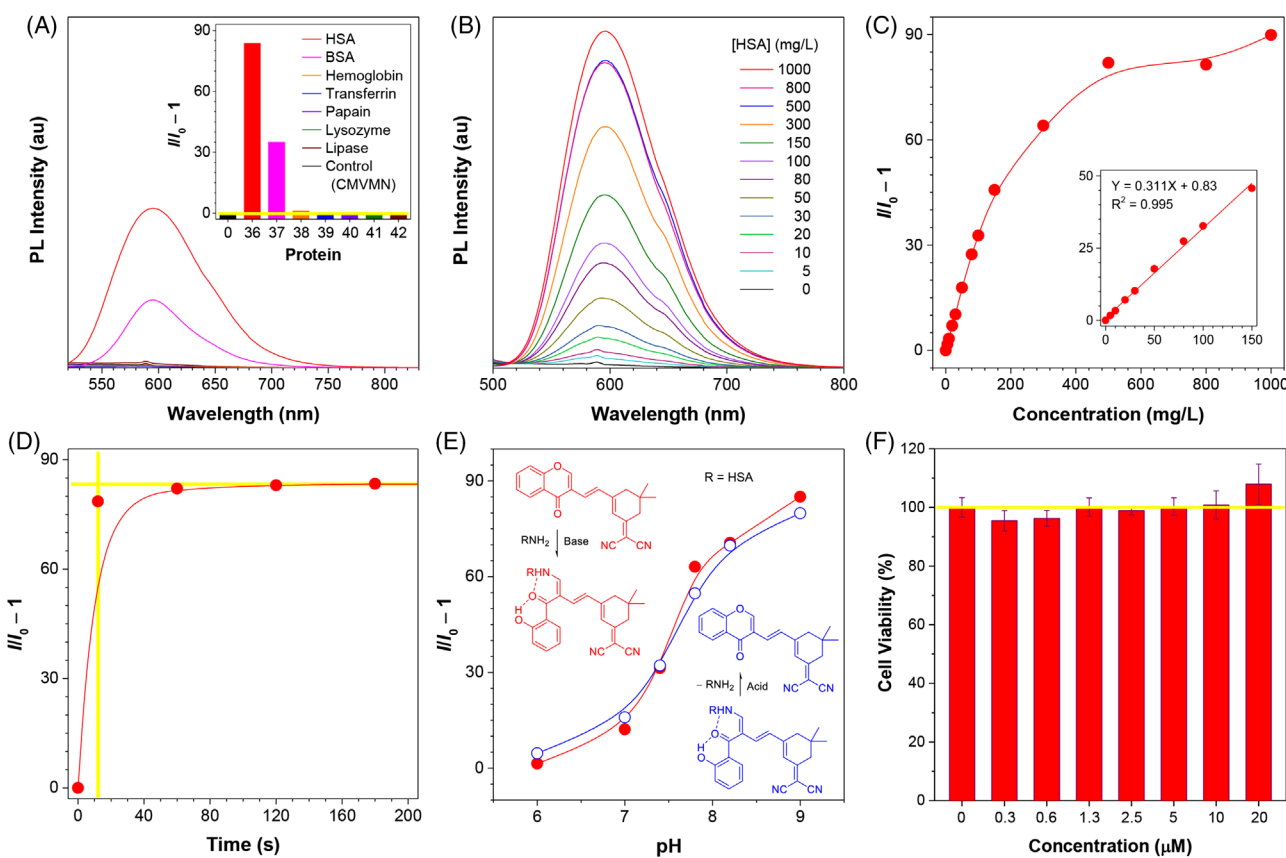


FIGURE 6 (A) PL spectra and (inset) relative fluorescence intensity ($I/I_0 - 1$) of CMVMN (10 μ M) in the presence of various protein (1 mg/mL) in PBS. Protein: [(0) CMVNM (control)], (36) HSA, (37) BSA, (38) hemoglobin, (39) transferrin, (40) papain, (41) lysozyme, (42) lipase. (B) Change in PL spectrum of CMVMN upon addition of different concentration of HSA. (C) Plot of ($I/I_0 - 1$) vs. concentration of HSA [HSA]. Inset: Linear fitting curve of ($I/I_0 - 1$) toward [HSA]. (D) Time course of amination of CMVMN with HSA. (E) Effect of pH on the reaction of CMVMN with HSA: amination at high pH and de-amination at low pH. (F) Effect of CMVMN on the cell viability of A375. Data shown were the mean \pm standard deviation of five separate measurements. $\lambda_{\text{ex/em}} = 480/595$ nm

as good as HSA. For the same reason, hemoglobin was found to be not reactive with CMVMN (Figure S24). However, other proteins (transferrin, papain, lysozyme, and lipase) were found not only unable to form stable complex with CMVMN, but also none of the arginine or lysine exhibit around the possible binding sites (Figures S25–S28). On the other hand, the reaction solution of CMVMN and HSA showed an absorption peak at 487 nm (Figure S29), which was in accordance with that of the amination products of CMVMN (Figure 2A). Thus, CMVMN can efficiently recognize and capture primary amino groups inside HSA. Even though the amination of CMVMN with specific amino acids (lysine and arginine) was applied for protein labeling, its efficiency is highly associated with the hydrophobic cleft of proteins. This offers a new approach for specific protein labeling.

Subsequently, quantitative analysis of HSA was performed. The fluorescence gradually increased upon addition of HSA and a good linear curve was obtained at a concentration range of 0–150 mg/L (Figure 6B and 6C), from which a detection limit of 1.2 mg/L was calculated. Also, quantitative analysis of BSA could be realized (Figure S30). Notably, the fluorescence “turn-on” response for HSA occurred within 10 s and its intensity nearly reached a plateau (Figure 6D), revealing the fast rate of amination. Moreover, a pH-dependent reactivity similar to that of lysine and arginine was detected for HSA (Figure 6E), but when lowering the pH, the fluorescence dropped rapidly and its value was close to that of the original state (Figure 6E), suggesting of

the occurrence of the deamination. Herein, tunable biolabeling of proteins in physiological pH conditions was realized by CMVMN, and it could be further applied for damage-free dynamic monitoring of proteins.

2.7 | Cell imaging and mitochondria staining

MTT assay was conducted and no considerable influence on cell viability was detected for CMVMN (Figure 6F and Figure S31). Also, a bright fluorescence of CMVMN was observed in A375 cells within 5 min and the fluorescence intensity reached a plateau 15 min later (Figure 7A), indicating the good biocompatibility and high reactivity of CMVMN in cells. Then, co-localization experiments with Mito-tracker green were conducted and a good Pearson’s colocalization coefficient of 0.94 was calculated (Figure 7B), which suggested that CMVMN is predominantly lighted up in mitochondria. A similar phenomenon was observed for C2C12 cells (Figure 7B and Figure S32), verifying the potential of CMVMN for mitochondria-staining. Since the amination process of CMVMN was pH-dependent and mitochondria happened to be slightly alkaline,^[64,65] CMVMN was partially restricted in mitochondria via amination and then lighted up.

In view of the high reactivity between CMVMN and HSA, it became notable for the performance of CMVMN in cells with abundant HSA. A variety of major plasma

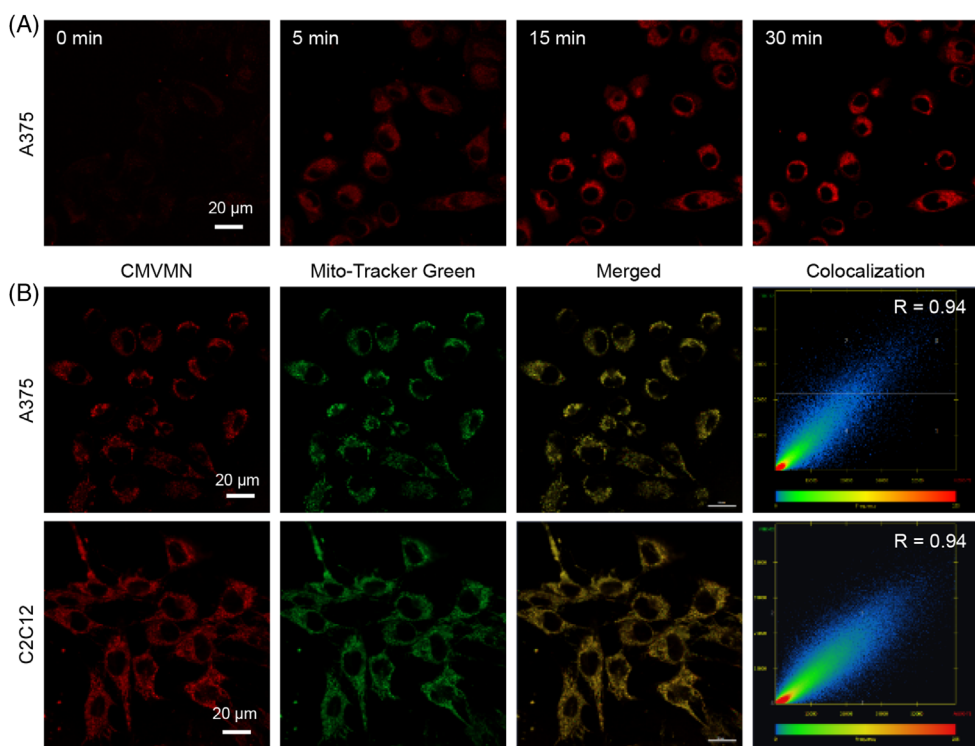


FIGURE 7 (A) Fluorescence images of A375 cells incubated with CMVMN (10 μ M). (B) Confocal microscopic images of A375 cells and C2C12 cells stained with CMVMN (10 μ M) and colocalization with Mito-Tracker Green (1 μ M). R = Pearson's coefficient

proteins, including albumin, were secreted in liver cells.^[66,67] Likely, the existence of HSA in cytoplasmic matrix and other organelles would induce a relatively high fluorescent signal outside of mitochondria for liver cells. To have a better vision of the co-localization efficiency, 3D z-stack imaging was obtained. The calculated Pearson's co-localization coefficient was good for C2C12 cells (0.90) (Figure S33) again, but became attenuated but tolerable (0.69–0.71) for liver cells, indicating the amination of CMVMN with HSA in liver cells. Additionally, a good mitochondria-staining ability was witnessed for A549 cells as expected. Hence, the pH-dependent reactivity of CMVMN made it a promising mitochondria-staining probe and other reactive proteins like HSA did exist in mitochondria for CMVMN. On the other hand, the fluorescence intensity in liver cells (HepG2 cells and L-02 cells) was found to be not significantly enhanced compared with that of C2C12 cells and A549 cells (Figure S34). Also, the mitochondria isolated from C2C12 cells induced an obvious enhancement in fluorescent signal after mixing with CMVMN (Figure S35). These further verified our conjecture of the existence of reactive proteins in mitochondria for amination of CMVMN. In previous works, special functional groups like pyridinium and triphenylphosphonium salt were needed to incorporate into luminogens to make them positively charged to target the mitochondria.^[68–70] Thus, CMVMN was a neutral molecule with mitochondria staining ability. Undoubtedly, it provided a new paradigm for designing mitochondria staining probes.

3 | CONCLUSION

The activated chromone derivative CMVMN reported in this paper filled the gap of selective bioconjugation for native

primary amine groups. Its reaction with primary amines was fast, efficient and highly selective in both solution and cells, and could be followed by the intense fluorescence “turn-on” signal. The combination of experimental results and theoretical calculations showed that both steric effect and the intramolecular hydrogen bonding between the carbonyl and NH groups were the cause for the high selectivity of CMVMN toward primary amines. Also, the AIE-active property of CMVMN made it suitable for solid-state sensing of amine vapors and printing process with a good performance in PA diffusion and leakage model. Moreover, CMVMN displayed a good mitochondria-staining property due to its pH-dependent reactivity with primary amines, which provided a new insight into the design of organelle-staining probes. To our knowledge, CMVMN was an example of scarcity for selective bioconjugation of primary amines in situ and it was also a neutral molecule with mitochondria-staining ability. It was anticipated that the present results would not only promote the development of chemoselective reactions in chemistry, but also offers new possibilities in biology.

ACKNOWLEDGMENTS

We are grateful for the financial support from the National Natural Science Foundation of China (21788102), the Research Grants Council of Hong Kong (16307020, 16306620, 16305518, N_HKUST609/19, C6009-17G, and C6014-20w), the Innovation and Technology Commission (ITC-CNERC14SC01 and ITCPD/17-9), and the Natural Science Foundation of Guangdong Province (201913121205002).

CONFLICT OF INTEREST

The authors declare that there is no conflict of interest regarding the publication of this article.

ORCIDXinyuan He  <https://orcid.org/0000-0002-4876-1656>Ben Zhong Tang  <https://orcid.org/0000-0002-0293-964X>**REFERENCES**

- H. W. Liu, K. Li, X. X. Hu, L. Zhu, Q. Rong, Y. Liu, X. B. Zhang, J. Hasserodt, F. L. Qu, W. Tan, *Angew. Chem. Int. Ed.* **2017**, *56*, 11788.
- S. S. Nguyen, J. A. Prescher, *Nat. Rev. Chem.* **2020**, *4*, 476.
- G. U. Nienhaus, *Angew. Chem. Int. Ed.* **2008**, *47*, 8992.
- J. A. Prescher, C. R. Bertozzi, *Nat. Chem. Biol.* **2005**, *1*, 13.
- H. C. Hang, C. Yu, D. L. Kato, C. R. Bertozzi, *Proc. Natl. Acad. Sci.* **2003**, *100*, 14846.
- X. Fan, J. Li, P. R. Chen, *Natl. Sci. Rev.* **2017**, *4*, 300.
- D. M. Patterson, L. A. Nazarova, B. Xie, D. N. Kamber, J. A. Prescher, *J. Am. Chem. Soc.* **2012**, *134*, 18638.
- J. Luo, Q. Liu, K. Morihiko, A. Deiters, *Nat. Chem.* **2016**, *8*, 1027.
- Y. Li, Z. Lou, H. Li, H. Yang, Y. Zhao, H. Fu, *Angew. Chem. Int. Ed.* **2020**, *59*, 3671.
- M. Grammel, H. C. Hang, *Nat. Chem. Biol.* **2013**, *9*, 475.
- T. Peng, H. C. Hang, *J. Am. Chem. Soc.* **2016**, *138*, 14423.
- A. Godinat, A. A. Bazhin, E. A. Goun, *Drug Discov. Today* **2018**, *23*, 1584.
- J. L. Klockow, K. S. Hettie, T. E. Glass, in *Comprehensive Supramolecular Chemistry II*, Elsevier, New York **2017**, pp. 447–467.
- G. Barbarella, *Chem. Eur. J.* **2002**, *8*, 5072.
- A. R. Morales, K. J. Schafer-Hales, A. I. Marcus, K. D. Belfield, *Bioconjugate Chem.* **2008**, *19*, 2559.
- R. Jia, W. Tian, H. Bai, J. Zhang, S. Wang, J. Zhang, *Nat. Commun.* **2019**, *10*, 795.
- B. J. C. Quah, H. S. Warren, C. R. Parish, *Nat. Protoc.* **2007**, *2*, 2049.
- D. Wang, J. Fan, X. Gao, B. Wang, S. Sun, X. Peng, *J. Org. Chem.* **2009**, *74*, 7675.
- L. Zhang, Y. Cheng, J. Lei, Y. Liu, Q. Hao, H. Ju, *Anal. Chem.* **2013**, *85*, 8001.
- M. Adamczyk, J. R. Fishbaugh, K. J. Heuser, *Bioconjugate Chem.* **1997**, *8*, 253.
- H. Zhao, P. Theato, *Polym. Chem.* **2013**, *4*, 891.
- S. Jeon, T. I. Kim, H. Jin, U. Lee, J. Bae, J. Bouffard, Y. Kim, *J. Am. Chem. Soc.* **2020**, *142*, 9231.
- G. J. Mohr, *Anal. Bioanal. Chem.* **2006**, *386*, 1201.
- A. R. Longstreet, M. Jo, R. R. Chandler, K. Hanson, N. Zhan, J. J. Hrudka, H. Matoussi, M. Shatruk, D. T. McQuade, *J. Am. Chem. Soc.* **2014**, *136*, 15493.
- A. M. ElSohly, M. B. Francis, *Acc. Chem. Res.* **2015**, *48*, 1971.
- A. D. Guo, D. Wei, H. J. Nie, H. Hu, C. Peng, S. T. Li, K. N. Yan, B. S. Zhou, L. Feng, C. Fang, M. Tian, R. Huang, X. H. Chen, *Nat. Commun.* **2020**, *11*, 5472.
- X. Hu, X. Zhao, B. He, Z. Zhao, Z. Zheng, P. Zhang, X. Shi, R. T. K. Kwok, J. W. Y. Lam, A. Qin, B. Z. Tang, *Research* **2018**, 3152870.
- V. A. Zagorevskii, É. K. Orlova, I. D. Tsvetkova, V. G. Vinokurov, V. S. Troitskaya, S. G. Rozenberg, *Chem. Heterocycl. Compd.* **1971**, *7*, 675.
- G. P. Ellis, I. M. Lockhart, in *The Chemistry of Heterocyclic Compounds, Chromenes, Chromanones, and Chromones*, Vol. 31, Wiley-VCH, New York **2007**, pp. 1–1196.
- D. S. Kemp, G. Hanson, *J. Org. Chem.* **1981**, *46*, 4971.
- P. J. L. Bell, P. Karuso, *J. Am. Chem. Soc.* **2003**, *125*, 9304.
- V. Y. Sosnovskikh, V. S. Moshkin, M. I. Kodess, *Tetrahedron Lett.* **2009**, *50*, 6515.
- V. O. Iaroshenko, S. Mkrtchyan, A. Gevorgyan, T. Grigoryan, A. Villinger, P. Langer, *RSC Adv.* **2015**, *5*, 28717.
- A. S. Badran, N. M. El-Gohary, M. A. Ibrahim, S. H. Hashiem, *J. Heterocycl. Chem.* **2020**, *57*, 2570.
- D. Cao, Z. Liu, P. Verwilst, S. Koo, P. Jangjili, J. S. Kim, W. Lin, *Chem. Rev.* **2019**, *119*, 10403.
- D. Ding, K. Li, B. Liu, B. Z. Tang, *Acc. Chem. Res.* **2013**, *46*, 2441.
- J. Luo, Z. Xie, J. W. Lam, L. Cheng, H. Chen, C. Qiu, H. S. Kwok, X. Zhan, Y. Liu, D. Zhu, B. Z. Tang, *Chem. Commun.* **2001**, *18*, 1740.
- J. Liang, B. Z. Tang, B. Liu, *Chem. Soc. Rev.* **2015**, *44*, 2798.
- J. Yang, Z. Chi, W. Zhu, B. Z. Tang, Z. Li, *Sci. China Chem.* **2019**, *62*, 1090.
- Q. Li, Z. Li, *Sci. China Mater.* **2020**, *63*, 177.
- L. Tu, Y. Xie, Z. Li, B. Z. Tang, *SmartMat* **2021**, *2*, 326.
- J. Yang, M. Fang, Z. Li, *Aggregate* **2020**, *1*, 6.
- Z. Liu, Q. Wang, Z. Zhu, M. Liu, X. Zhao, W. H. Zhu, *Chem. Sci.* **2020**, *11*, 12755.
- H. Li, H. Kim, J. Han, V. Nguyen, X. Peng, J. Yoon, *Aggregate* **2021**, *2*, e51.
- Y. Dong, J. W. Lam, A. Qin, Z. Li, J. Sun, H. H. Sung, I. D. Williams, B. Z. Tang, *Chem. Commun.* **2007**, *40*.
- M. Yamaguchi, S. Ito, A. Hirose, K. Tanaka, Y. Chujo, *Mater. Chem. Front.* **2017**, *1*, 1573.
- Z. Wang, T. Wang, C. Zhang, M. G. Humphrey, *Phys. Chem. Chem. Phys.* **2017**, *19*, 12928.
- Z. Zhao, H. Zhang, J. W. Y. Lam, B. Z. Tang, *Angew. Chem. Int. Ed.* **2020**, *59*, 9888.
- W. Chen, A. Pacheco, Y. Takano, J. J. Day, K. Hanaoka, M. Xian, *Angew. Chem., Int. Ed.* **2016**, *55*, 9993.
- H. Si, K. Wang, B. Song, B. Z. Tang, *Polym. Chem.* **2020**, *11*, 2568.
- A. O. Konuray, X. Fernández-Francos, X. Ramis, *Polym. Chem.* **2020**, *8*, 5934.
- S. Singha, Y. W. Jun, S. Sarkar, K. H. Ahn, *Acc. Chem. Res.* **2019**, *52*, 2571.
- L. Shi, Y. Fu, C. He, D. Zhu, Y. Gao, Y. Wang, Q. He, H. Cao, J. Cheng, *Chem. Commun.* **2014**, *50*, 872.
- Y. Fu, W. Xu, Q. He, J. Cheng, *Sci. China Chem.* **2016**, *59*, 3.
- A. Gupta, *ChemistrySelect* **2019**, *4*, 12848.
- C. C. Winterbourn, *Arch. Biochem. Biophys.* **2016**, *595*, 68.
- E. C. Vermisoglou, P. Jakubec, A. Bakandritsos, V. Kupka, M. Pykal, V. Šedajová, J. Vlček, O. Tomanec, M. Scheibe, R. Zbořil, M. Otyepka, *Chem Sus Chem* **2021**, *14*, 3904.
- O. Koniev, A. Wagner, *Chem. Soc. Rev.* **2015**, *44*, 5495.
- J. N. deGruyter, L. R. Malins, P. S. Baran, *Biochemistry* **2017**, *56*, 3863.
- V. Grundler, K. Gademann, *ACS Med. Chem. Lett.* **2014**, *5*, 1290.
- T. Kouzarides, *Cell* **2007**, *128*, 693.
- E. L. Greer, Y. Shi, *Nat. Rev. Genet.* **2012**, *13*, 343.
- P. Wei, Z. Li, J. X. Zhang, Z. Zhao, H. Xing, Y. Tu, J. Gong, T. S. Cheung, S. Hu, H. H. Y. Sung, I. D. Williams, R. T. K. Kwok, J. W. Y. Lam, B. Z. Tang, *Chem. Mater.* **2019**, *31*, 1092.
- J. Casey, S. Grinstein, J. Orlowski, *Nat. Rev. Mol. Cell Biol.* **2010**, *11*, 50.
- M. Benčina, *Sensors* **2013**, *13*, 16736.
- R. Zhao, T. Jia, H. Shi, C. Huang, *J. Mater. Chem. B* **2019**, *7*, 2782.
- G. J. van der Vusse, *Drug Metab. Pharmacokinet.* **2009**, *24*, 300.
- Q. Hu, M. Gao, G. Feng, B. Liu, *Angew. Chem. Int. Ed.* **2014**, *53*, 14225.
- A. R. Sarkar, C. H. Heo, L. Xu, H. W. Lee, H. Y. Si, J. W. Byun, H. M. Kim, *Chem. Sci.* **2016**, *7*, 766.
- N. E. Choi, J. Y. Lee, E. C. Park, J. H. Lee, J. Lee, *Molecules* **2021**, *26*, 217.

SUPPORTING INFORMATION

Additional supporting information can be found online in the Supporting Information section at the end of this article.

How to cite this article: X. He, H. Xie, L. Hu, P. Liu, C. Xu, W. He, W. Du, S. Zhang, H. Xing, X. Liu, H. Park, T. S. Cheung, M.-H. Li, R. T. K. Kwok, J. W. Y. Lam, J. Lu, B. Z. Tang, *Aggregate* **2022**, e239. <https://doi.org/10.1002/agt2.239>